Appl. Phys. B 86, 561–566 (2007)
DOI: 10.1007/s00340-006-2503-8

Applied Physics B
Lasers and Optics

L. GALLMANN[1,2,✉]
T. PFEIFER[1,2]
P.M. NAGEL[1,2]
M.J. ABEL[1,2]
D.M. NEUMARK[1,2]
S.R. LEONE[1,2]

Comparison of the filamentation and the hollow-core fiber characteristics for pulse compression into the few-cycle regime

[1] Departments of Chemistry and Physics, University of California, Berkeley, CA 94720, USA
[2] Chemical Sciences Division, Lawrence Berkeley National Laboratory, Berkeley, CA 94720, USA

Received: 18 July 2006/Revised version: 23 October 2006
Published online: 5 December 2006 •

ABSTRACT The gas-filled hollow-core fiber compression and the optical filamentation technique are compared experimentally in a parameter regime suitable for intense few-cycle pulse generation. In particular, pointing stability, spectral properties, and spatial chirp are investigated. It is found that in the case of filamentation, the critical parameter for pointing stability is gas pressure inside the generation cell whereas for the hollow-core fiber it is alignment that plays this role. The hollow-core fiber technique yields spectra that are better suited for chirped-mirror pulse compression whereas filamentation offers higher throughput and prospects for easy-to-implement self-compression. We present spectral phase interferometry for direct electric-field reconstruction (SPIDER) measurements that directly show the transition in the spectral phase of the output continua into the self-compression regime as the gas pressure is increased.

PACS 42.65.Re; 42.65.Jx; 42.65.Tg

1 Introduction

Many applications in ultrafast optical science require intense few-cycle laser pulses. Such applications include high-field laser science and, in particular, single attosecond pulse generation [1]. Most commonly, intense few-cycle pulses are generated either in noncollinear optical parametric amplifiers [2] or by compression of the continuum output from a rare-gas filled hollow-core fiber [3, 4]. Recently, a new method for the generation of intense few-cycle pulses has been found. This technique is based on optical filamentation of an amplified laser beam in a rare gas [5, 6]. Optical filamentation is the self-guiding of a beam through a dynamical balance between the focusing action of the Kerr effect and the defocusing action of diffraction and the plasma created by the intense beam [7]. Simultaneously, the Kerr nonlinearity also acts to broaden the pulse spectrum during propagation in the filament through self-phase modulation. Similar to the traditional hollow-core fiber technique, the continuum output can be compressed after the filament using chirped mirrors or other dispersion compensation methods [5]. In addition, self-compression may be observed in certain operation regimes [5].

✉ Fax: +41 44 633 10 59, E-mail: gallmann@phys.ethz.ch

The filamentation approach is an attractive alternative for several reasons. First, its experimental arrangement is simpler than that of other methods. Second, due to the absence of a waveguide and its associated coupling losses, significantly higher throughput can be obtained compared with the hollow-core fiber technique [5]. Third, optical filamentation offers the exciting prospects of self-compression into the single-cycle pulse duration regime [8, 9]. Self-compression from 45 fs down to 7.8 fs of 2 mJ pulses from a Ti:sapphire amplifier system has recently been demonstrated experimentally [10]. For completeness, we note that self-compression has also been predicted and demonstrated for an arrangement using a hollow-core fiber operated above the ionization threshold of the gas medium [11]. For this approach, self-compression was explained by a three-dimensional interplay between effects due to the generated plasma and the waveguide. However, scalability of that approach including its possible extension into the single-cycle regime has yet to be shown.

In this paper, we present a detailed experimental investigation of the most important performance parameters of the hollow-core fiber and filamentation techniques under conditions representative of few-cycle pulse generation. The latter implies that this study is limited to the single-filament regime in the case of optical filamentation. Break-up into multiple filaments is observed at high intensities and/or gas pressures [7]. Since most experiments with few-cycle pulses require clean and stable beam profiles, multiple filaments are usually not considered for these applications because they fail to provide these desired properties. The performance parameters that were investigated include the beam pointing stability and beam profiles in and out of focus, spatial chirp, and spectral phase. Measurements were performed for a range of gas pressures in order to understand the pressure scaling of various properties in each approach and to find the most stable operating conditions.

2 Experimental setup and parameters

For all of the following experiments, a commercial multi-pass Ti:sapphire amplifier system (Femtolasers FemtoPower Pro) capable of producing ∼ 25-fs pulses was used to provide the intense driver pulses. This system delivers pulses centered at 780 nm wavelength with ∼ 0.8 mJ pulse energy and a repetition rate of 3 kHz. The hollow-core fiber and the

filamentation cells were set up in parallel at approximately the same distance from the amplifier system to assure comparable conditions at their input. Both generation cells were operated such that they yield the best performance in view of few-cycle pulse generation. As a result, the hollow-core fiber with an inner diameter of 250 μm was filled with Ne gas to minimize unwanted plasma formation, whereas the filamentation cell, in which a certain amount of plasma formation is required, was filled with Ar gas. About 0.7 mJ of the original pulse energy arrived at the input of the generation cells. An energy throughput of ∼ 50% was observed for the hollow-core fiber cell with no significant pressure dependence over the range that was investigated, while ∼ 95% was measured for filamentation in the relevant 1.0–1.6 bar range. A 1 m focal length mirror was used for optimum coupling into the hollow-core fiber, whereas a 1.5 m focal length mirror was found to yield the best performance in the case of filamentation. For both techniques, the pre-chirp or compression of the input pulses was chosen to produce maximum spectral broadening. The output beams from both cells were collimated using a 1.5 m focal length mirror. The only parameter that was varied during the following measurements was the pressure of the rare gas. Gas pressures were adjusted between 0 bar and 2 bar for both techniques. Higher gas pressures were not explored due to the risk of fracturing the 0.5 mm thick fused silica windows used as the input and output ports of the gas cells. However, it was found that optimum performance can be achieved in this gas pressure range for both methods.

On the diagnostics side, a charge-coupled device (CCD) camera was used to monitor the beam profiles in and out of focus. Series of images from the same camera were analyzed to yield information on the beam pointing stability. The pulse spectra were recorded with a HR2000 spectrometer from Ocean Optics Inc. and corrected for spectral sensitivity variations using a black-body calibration lamp. Spatial chirp of the output beams was investigated by aperturing out certain parts of the beam with a small iris aperture and acquiring the transmitted light with the spectrometer. A broadband spectral phase interferometry for direct electric-field reconstruction (SPIDER, [12, 13]) setup provided the spectral phase information.

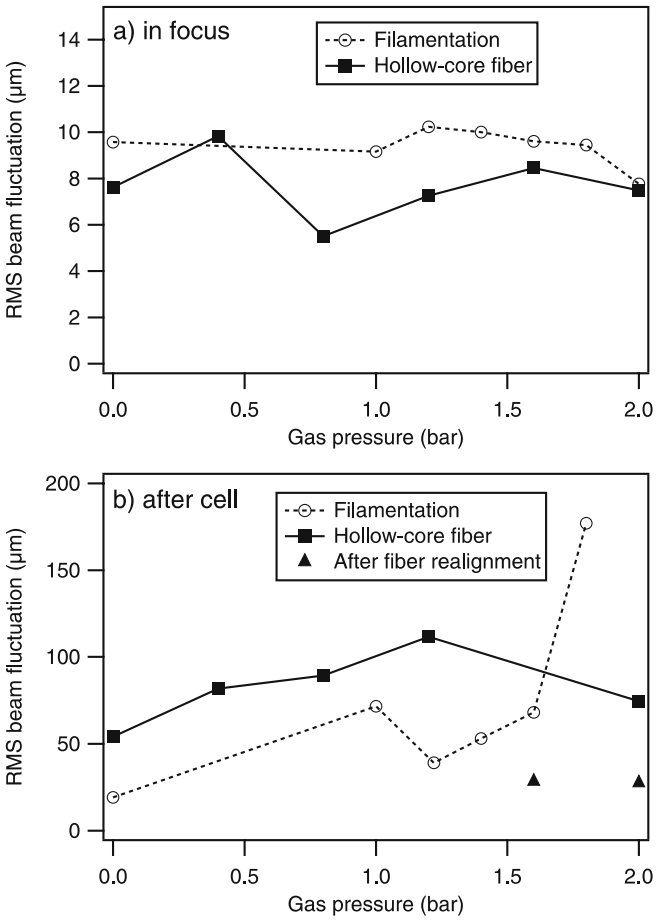

FIGURE 1 Root-mean-square of the beam centroid fluctuations observed with a CCD on a white paper screen as a function of gas pressure. The data points in (**a**) have been obtained in the focal plane of a 1.5 m focal length mirror used for refocusing the collimated output beam. The data shown in (**b**) was measured ∼ 1.2 m after the estimated end of the filament and ∼ 0.9 m after the end of the hollow-core fiber. The data points for the filamentation technique are shown as *circles* connected by a *dashed line*. The hollow-core fiber points are represented by *filled boxes* connected by a *solid line*. The *filled triangles* in (**b**) show the pointing stability obtained with the hollow-core fiber technique after reoptimization of the coupling into the fiber

3 Pointing stability

One of the main concerns generally associated with optical filamentation is its potentially lower beam pointing stability as compared to the hollow-core fiber technique. In the case of the fiber, the confinement by the waveguide acts to stabilize the output beam. Filamentation does not benefit from such an effect. Even worse, it was suspected that instabilities in the input beam may even be further amplified by the filament's fragile dynamical balance between plasma and Kerr effect. However, as it was shown recently, the pointing stability of a filament after a focusing lens can be similar to that of the input beam [6].

We performed an extensive investigation of beam pointing stability as a function of gas pressure, transverse direction, and position along the beam. Each data point in Fig. 1 was obtained by acquiring fifty images of the beam on a white paper screen using a CCD camera. The images were taken over a time interval with a duration of 20 to 25 s. The root-mean-square (rms) beam fluctuation was determined from the statistics of the centroids of the squared intensity distributions. The square of the images was taken to reduce the influence of low intensity light on the determination of the beam center. A stable low intensity halo as is typically observed with filamentation would otherwise partially mask the actual fluctuations of the filament when using a purely linear centroid method.

The focal plane measurements shown in Fig. 1 were taken after refocusing the collimated output beam using a 1.5 m focal length concave mirror. In the case of filamentation care had to be taken to ensure that the screen was located in the actual focal plane since the pressure dependence of the filament length impacts beam collimation. No systematic pressure dependence of the beam stability in the focal plane was found for both pulse generation techniques. For comparison, the actual beam diameters in the focus change from 140 μm full-width at half maximum (FWHM) at 0 bar to 250 μm at 1.4 bar and 310 μm at 2.0 bar in the case of the filamentation and from

150 μm at 0 bar to 190 μm at 2 bar in the case of the hollow-core fiber method.

On the other hand, visual inspection of the filamentation beam on a screen positioned in the unfocused beam after the generation cell already clearly shows how the beam suddenly stabilizes once the pressure reaches the point of single filament onset which takes place at ∼ 1 bar of Ar pressure. The filament beam remains stable within a pressure window of several 100 mbar and then becomes unstable again when the pressure is high enough to cause break-up of the single filament. In our case, filament break-up was observed for pressures beyond 1.6 bar. Although higher spectral bandwidths are obtained for higher pressures with corresponding calculated transform limits of down to < 2 fs at 2 bar Ar, the cleanest and most stable filament beam is observed at gas pressures of around 1.4 to 1.2 bar with corresponding transform limited bandwidths of 3 to 5 fs.

This clear pressure dependence is also reflected in the beam stability monitored ∼ 1.2 m after the estimated end of the filament (see Fig. 1). In the case of the hollow-core fiber, no significant pressure dependence is found with the screen positioned ∼ 0.9 m after the fiber end. The lower lying data points at 1.6 bar and 2.0 bar gas pressure were obtained after reoptimization of the coupling into the capillary. While the throughput of the capillary was changed only slightly by this realignment, there was a substantial improvement in pointing stability. This is explained by the fact that the excitation and suppression of higher spatial modes depends critically on the quality of the coupling of the input beam into the waveguide. Fluctuating contributions of higher modes to the output beam profile affect the stability of the beam. For the fiber, a transform limited bandwidth of 4.1 fs is found at 2 bar of Ne pressure with no obvious deterioration in beam quality.

It was recently demonstrated that the pointing stability of the filament can be further improved by incorporating a circular spatial phase mask into the beam in front of the filamentation chamber [14]. Another benefit of this technique is that the phase mask can also be used to enhance the spectral bandwidth of the output beam [14]. However, in this paper we limit the discussion to the conventional approach of filamentation using no phase mask.

From these findings, one may conclude that optical filamentation and the hollow-core fiber technique yield comparable pointing stability and spectral bandwidths at their optimum gas pressure. While the performance of filamentation depends more critically on gas pressure, the hollow-core fiber approach is more sensitive to alignment. The higher alignment sensitivity of the hollow-core fiber technique can be explained by the suppression or excitation of higher order spatial modes depending on the coupling into the fiber.

4 Spectral properties

Besides the pure spectral bandwidths already briefly discussed in the previous paragraph, the actual spectral energy distribution, the amount of spatial chirp and the spectral phase are of particular interest. With regard to the spectral energy distribution, it is generally found that the spectra generated with filamentation usually possess a long tail towards short wavelengths due to interaction with the plasma, whereas the hollow-core fiber yields the more box-shaped spectra typical for dominant self-phase modulation (SPM) and those spectra extend slightly further to long wavelengths. Figure 2 depicts two typical spectra on a logarithmic scale. The same spectra are shown again in Fig. 3 on a linear scale. The box shape is considered an advantage if chirped mirrors are used for performing the pulse compression because more spectral energy can be fit into the limited bandwidth of these optics. On the other hand, the higher energy content at short wavelengths found in the filamentation spectra is often sufficient to extend the overall frequency span beyond one optical octave, which allows for simpler implementation of carrier-envelope phase tracking schemes [15, 16].

The spectral phase interferometry for direct electric-field reconstruction (SPIDER, [12, 13]) technique was used to measure how the spectral phase changes upon increasing the gas pressure. In order to isolate the contribution from changing the gas pressure alone, the difference between the spectral phase at two neighboring gas pressure values was taken. This way all pressure independent phase contributions such as those caused by the dispersion of the gas cell windows or other optical elements cancel out. The curves plotted in Fig. 3 represent the difference between the spectral phase measured at the higher indicated pressure minus the spectral phase measured at the lower value. Each curve has been obtained by averaging the results from three independent SPIDER measurements per pressure setting.

From a purely linear optical point of view, one would expect those curves to be dominantly quadratic with positive curvature due to the material dispersion introduced by the added gas. In addition, the spectral phase differences would only depend on the pressure change between the two SPIDER measurements and not on the absolute values of the gas pressure. Although one clearly observes the positive curvature in the hollow-fiber data, the curvature systematically increases with pressure. From the length of the gas cell, the material contribution from the added 0.4 bar of Ne can be calculated to

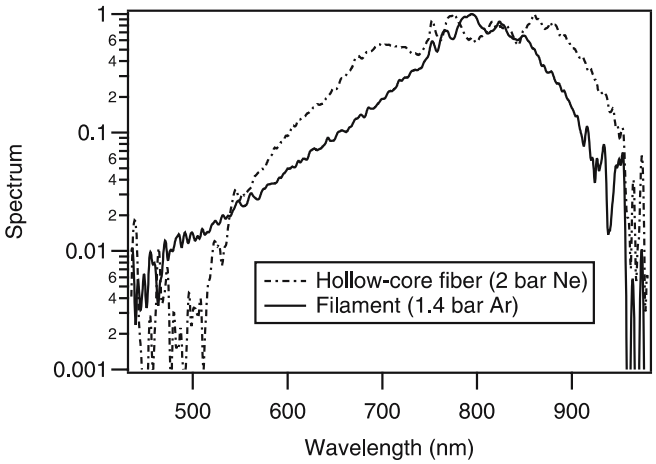

FIGURE 2 Typical spectra generated using the hollow-core fiber and the optical filamentation technique. The two spectra have been normalized to one at their maximum spectral power density. The spectrum generated with the hollow-core fiber method (*dash-dotted line*) is more box-shaped and extends to slightly longer wavelengths than that produced by the filament (*solid line*). Filamentation spectra typically possess long wings slowly decaying towards the short wavelength side

amount to about 1.6 fs^2 at 780 nm wavelength [17]. The measured curvatures on the other hand increase from $\sim 1.9\,fs^2$ at the lowest pair of pressures to $\sim 12\,fs^2$ at medium pressure and finally to $\sim 34\,fs^2$ at the highest pressures. This increase in positive curvature is a manifestation of the increasing self-phase modulation experienced by the intense pulse propagating through the capillary [18].

In the case of filamentation, on the other hand, the curves in Fig. 3 change their sign with increasing pressure. This is believed to be due to an increasing phase contribution from the plasma. In fact, this change of sign can be understood as a manifestation of an effect that ultimately can be used to achieve self-compression of the filament. For our data set, the material dispersion contribution to the measured phase difference from adding 0.2 bar of Ar can be calculated to amount to about 8 fs^2 at 780 nm [17]. The measured curvatures change from $\sim 39\,fs^2$ at the lowest pair of pressures to $\sim -1.5\,fs^2$ at medium pressure and finally to $\sim -27\,fs^2$ at the highest pressures.

For some applications, it is also important to know how the spectral content varies along the transverse direction of the beam, i.e., how pronounced its spatial chirp is. Spatial chirp will also result in a transverse dependence of the temporal structure of the compressed pulses [19]. For such broadband beams, a spatial chirp is almost always present already as a natural result of free-space diffraction. However, with almost any technique for few-cycle pulse generation, one observes more significant and more structured spatial chirp than what would be expected from beam propagation alone. Figure 4 shows spatially resolved spectra obtained by scanning an iris aperture horizontally through the output beam generated by each of the two methods discussed in this paper. The iris aperture was 0.6 mm while the $1/e^2$ beam diameter of the hollow-fiber output was ~ 6 mm and that of the filamentation output was ~ 3.7 mm at the position of the iris. The scanning was performed ~ 1 m after the filament and fiber, re-

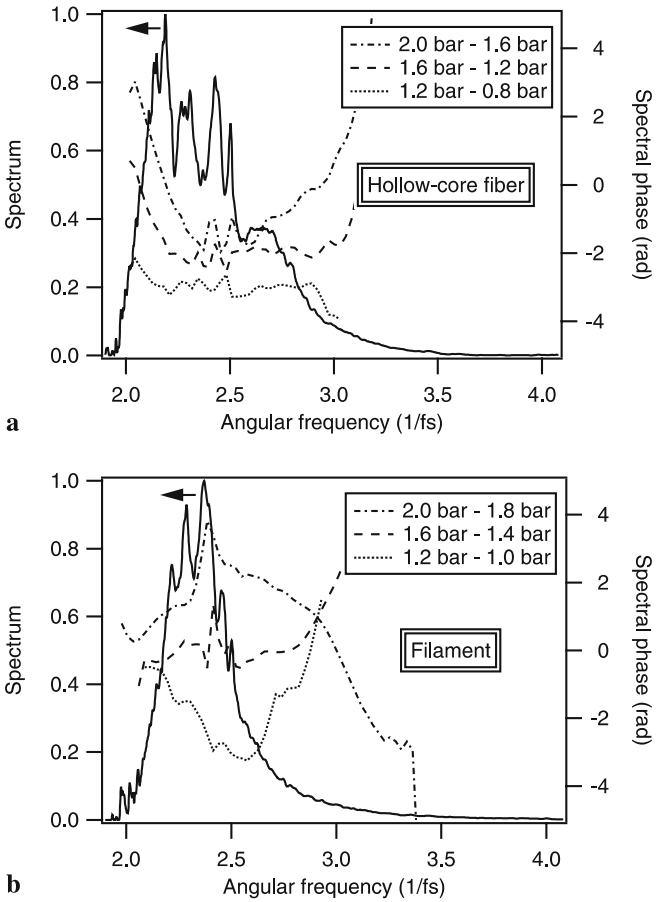

FIGURE 3 Spectra (*solid lines*) obtained at optimum operating conditions for both techniques and spectral phase variation with pressure. The spectra have been recorded using a gas pressure of 1.4 bar Ar in the case of filamentation and at a pressure of 2 bar Ne for the hollow-core fiber. The spectral phase plots have been obtained by taking SPIDER measurements at two different gas pressures and subtracting the lower pressure data set from the higher pressure data set. In the case of the hollow-core fiber technique shown in (**a**), the curvature of the phase becomes increasingly positive with pressure which is mainly a result of the stronger self-phase modulation at higher gas densities. The filamentation data displayed in (**b**) evolves towards increasing negative curvatures with increasing pressure. This behavior can be understood as direct evidence for the self-compression effect predicted in [8]

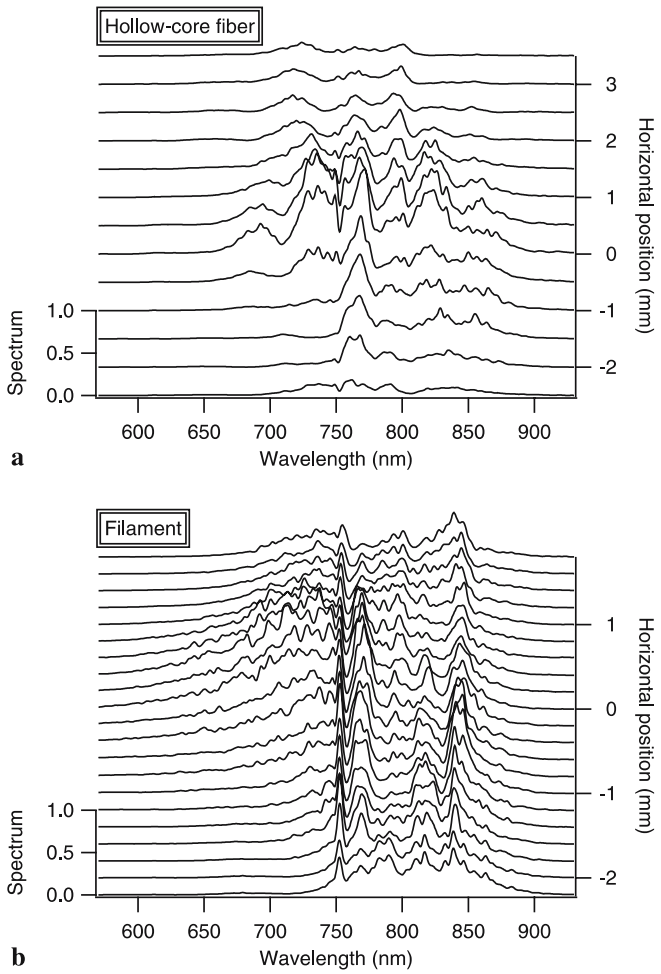

FIGURE 4 Spatial chirp of the output beams along the horizontal axis. The individual traces shown represent the spatially resolved spectral power density. Spatial resolution has been obtained by scanning a small aperture through the beam while recording the transmitted optical spectrum. Binomial smoothing has been applied to the spectra to remove high-frequency pixel-to-pixel noise which might distract from the actual more slowly varying spatial chirp. The spatial variation is about the same for all spectral components in the case of the hollow-core fiber shown in (**a**). For the filament data in (**b**), a pronounced change in the spatial distribution of the spectral content can be observed above 760 nm. Spatial chirp along the vertical axis is qualitatively the same

spectively, and the lateral scanning range was approximately one $1/e^2$ beam diameter around the estimated center of the beam. The results obtained for vertical scanning of the iris are qualitatively the same. For these measurements, 1.6 bar of Ar was used in the filamentation cell and 2.0 bar of Ne in the hollow-core fiber. For a better visualization of the spatial chirp, Fig. 5 shows the deviation of the spectra shown in Fig. 4 from the intensity-weighted average spectrum. In the case of the hollow-core fiber, the spatial chirp is relatively evenly distributed whereas the structure of the spatial chirp changes dramatically above 760 nm for the filamentation-based approach. In the latter case, the spectral content at shorter wavelength changes on a much shorter length scale while the long wavelength content remains almost constant over a wide range. This indicates a larger effective beam diameter for the longer wavelengths and a less Gaussian-like beam profile. The exact origin of this effect is not understood.

In an attempt to quantify the amount of spatial chirp present in the beams generated by the two methods, we calculated the transform limited pulse durations corresponding to each spectral slice shown in Fig. 4. This yields the lateral variation of pulse durations under the condition of optimum compression at each position, which is an aspect of spatial chirp that is particularly relevant for many few-cycle pulse applications. In the case of the hollow-core fiber technique, one finds that the transform limit remains almost constant for the center part and drops slightly towards the lower intensity wings of the beam. If evaluated over the $1/e^2$ diameter, one obtains an intensity-weighted average transform limit of 6.5 fs with a 0.4 fs intensity-weighted root-mean-square deviation across this part of the beam. For the filamentation approach, the shortest transform limits are found in the beam center, while they are considerably longer towards the wings. The same evaluation as for the hollow-core fiber was applied to the filament data, resulting in an average transform limited pulse duration of 4.8 fs with a weighted rms deviation of 0.9 fs. These results imply that the amount of spatial chirp is higher in the case of the filamentation technique and that it is crucial for this approach to utilize only the center part of the beam in order to obtain the shortest output pulses. The latter is in agreement with observations in [5] and, of course, limits the achievable throughput for applications requiring the shortest pulses.

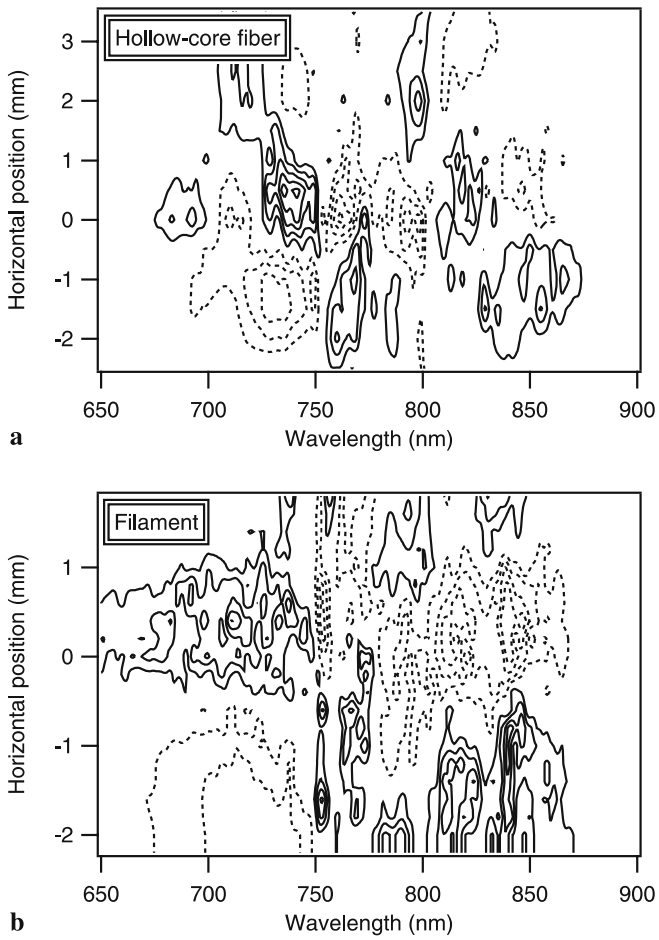

FIGURE 5 Deviation of the spectra shown in Fig. 4 from the intensity-weighted average (integrated) spectrum. Negative contours are shown as *dashed lines*, positive contours as *solid lines*. Both contour plots use the same contour levels. The structure of the spatial chirp is more homogeneous in the case of the hollow-core fiber, while spatial chirp is more pronounced and its structure changes from shorter to longer wavelengths in the case of filamentation

5 Conclusion

We performed an extensive experimental comparison of the filamentation and hollow-core fiber techniques for few-cycle pulse generation. The results show some advantages and weaknesses of either method. On one hand, the hollow-core fiber approach results in spectra that are better suited for chirped-mirror based pulse compression and produces beams of excellent quality over wide pressure ranges. Besides the well-known disadvantage of the coupling losses introduced by the fiber, one has to mention on the negative side that the properties of its output beam sensitively depend on alignment through possible excitation of unwanted higher spatial modes and may thus become subject to thermal drift. On the other hand, filamentation requires more careful control of gas pressures, but offers almost twice as much throughput as the capillary if there is no stringent requirement on lateral uniformity of the pulse duration. Our data confirm that pointing stability can be similar for the two techniques under the right experimental conditions.

While the hollow-core fiber technique is a well-established and proven method, optical filamentation for the generation of few-cycle pulses is a rather new research topic. One can expect that the latter technique will see various improvements and adaptations for specific applications as new effects are discovered. Particularly exciting are the prospects for self-compression into the single-cycle regime predicted for filamentation [8, 9]. This could become the easiest route to such pulse durations in the visible spectral region.

The particular type of application determines what pulse generation technique is the best choice to deliver the required performance. Nevertheless, pulse compression using single filaments in rare gases is definitely a promising addition to the previously existing few-cycle pulse generation methods. Many exciting results can be expected from this technique in the future.

ACKNOWLEDGEMENTS The authors acknowledge financial support of a MURI program from the Air Force Office of Scientific Research, contract No. FA9550-04-1-0242. Portions of the laboratory were supported by the Director, Office of Science, Office of Basic Energy Sciences, of the US Department of Energy under contract DE-AC02-05CH11231.

REFERENCES

1 M. Hentschel, R. Kienberger, C. Spielmann, G.A. Reider, N. Milosevic, T. Brabec, P. Corkum, U. Heinzmann, M. Drescher, F. Krausz, Nature **414**, 509 (2001)
2 A. Shirakawa, I. Sakane, M. Takasaka, T. Kobayashi, Appl. Phys. Lett. **74**, 2268 (1999)
3 M. Nisoli, S.D. Silvestri, O. Svelto, Appl. Phys. Lett. **68**, 2793 (1996)
4 M. Nisoli, S.D. Silvestri, O. Svelto, R. Szipöcs, K. Ferencz, C. Spielmann, S. Sartania, F. Krausz, Opt. Lett. **22**, 522 (1997)
5 C.P. Hauri, W. Kornelis, F.W. Helbing, A. Heinrich, A. Couairon, A. Mysyrowicz, J. Biegert, U. Keller, Appl. Phys. B **79**, 673 (2004)
6 C.P. Hauri, A. Guandalini, P. Eckle, W. Kornelis, J. Biegert, U. Keller, Opt. Express **13**, 7541 (2005)
7 A. Braun, G. Korn, X. Liu, D. Du, J. Squier, G. Mourou, Opt. Lett. **20**, 73 (1995)
8 A. Couairon, M. Franco, A. Mysyrowicz, J. Biegert, U. Keller, Opt. Lett. **30**, 2657 (2005)
9 A. Couairon, J. Biegert, C.P. Hauri, W. Kornelis, F.W. Helbing, U. Keller, A. Mysyrowicz, J. Mod. Opt. **53**, 75 (2006)
10 G. Stibenz, N. Zhavoronkov, G. Steinmeyer, Opt. Lett. **31**, 274 (2006)
11 N.L. Wagner, E.A. Gibson, T. Popmintchev, I.P. Christov, M.M. Murnane, H.C. Kapteyn, Phys. Rev. Lett. **93**, 173 902 (2004)
12 C. Iaconis, I.A. Walmsley, Opt. Lett. **23**, 792 (1998)
13 L. Gallmann, D.H. Sutter, N. Matuschek, G. Steinmeyer, U. Keller, C. Iaconis, I.A. Walmsley, Opt. Lett. **24**, 1314 (1999)
14 T. Pfeifer, L. Gallmann, M.J. Abel, D.M. Neumark, S.R. Leone, Opt. Lett. **31**, 2326 (2006)
15 H.R. Telle, G. Steinmeyer, A.E. Dunlop, J. Stenger, D.H. Sutter, U. Keller, Appl. Phys. B **69**, 327 (1999)
16 M. Mehendale, S.A. Mitchell, J.-P. Likforman, D.M. Villeneuve, P.B. Corkum, Opt. Lett. **25**, 1672 (2000)
17 S.A. Korff, G. Breit, Rev. Mod. Phys. **4**, 471 (1932)
18 G.P. Agrawal, *Nonlinear Fiber Optics* (Academic Press, London, 2001)
19 L. Gallmann, G. Steinmeyer, D.H. Sutter, T. Rupp, C. Iaconis, I.A. Walmsley, U. Keller, Opt. Lett. **26**, 96 (2001)